How can we detect and analyze traveling waves in human brain oscillations?

Anup Das[1], Erfan Zabeh[1,2], and Joshua Jacobs[1,3]

[1]Department of Biomedical Engineering

[2]Mortimer B. Zuckerman Mind Brain Behavior Institute

[3]Department of Neurological Surgery

Columbia University

New York, NY 10027

Corresponding author email address: ad3772@columbia.edu, joshua.jacobs@columbia.edu

Number of pages: 22

Number of figures: 4

Conflict of interest statement: The authors declare no competing financial interests.

Acknowledgements

We thank Drs. Uma Mohan and Honghui Zhang for technical assistance. This research was supported by a RISE award and an NSF CAREER award to J.J.

Abstract

The brain is a complex, interconnected network and the large-scale spatiotemporal coordination of neuronal activity is vital for cognition and behavior. Prior studies have proposed that traveling waves of brain oscillations are one mechanism that helps coordinate complex neuronal processes and are crucial for cognition. Traveling waves consist of oscillations that propagate progressively across the cortex and previous studies have shown that these waves play a foundational role for learning, memory processing, and memory consolidation and a range of other behaviors across multiple species. The prevalence of traveling waves in cognition thus indicates that spatiotemporal patterns of neuronal oscillations may coordinate multiple neuronal brain networks and impact behavior. Even though there are several different approaches for analyzing traveling waves using electrophysiological recordings, computational tools targeting the analysis and visualization and understanding of traveling waves are still rare. We briefly review the literature on human intracranial electroencephalography (iEEG), which has shown that traveling waves play an important role in cognition. We then describe a statistical methodology based on circular–linear regression for the detection and analysis of traveling waves from human electrophysiological oscillations. We hope that this approach will provide a more mechanistic understanding of the coordination of neurons across space and time.

Introduction

Prior research has shown that neuronal oscillations play a fundamental role for learning, memory processing, and consciousness in the brain across species (1, 2) (see also **Chapter 22**). Starting from the discovery of alpha frequency band (8-12 Hz) oscillations by Hans Berger in 1929 (3) in scalp electroencephalograhy (EEG) recordings in humans to the advent of invasive electrocorticogram recordings in 1949 by Jasper and Penfield in humans (4), oscillations are now widely believed to play an important role for spatiotemporal coordination among multiple brain networks (2). Growing evidence suggests that oscillations do not occur at individual neurons in an isolated way, rather they occur simultaneously across multiple neurons in a given small brain area or on a larger scale across multiple brain areas (5).

Oscillation-based temporal synchronization among neurons is a foundational mechanism for information transfer and coordination among neurons (2). These synchronization mechanisms are usually thought to involve zero-phase-lag synchronization among neurons, where phases of the recordings from multiple electrodes are temporally aligned (6). However, recent studies have found waves of electrical activity propagating across the cortex in the human brain (7-15). This was possible because of improved methods in analyzing simultaneous intracranial EEG (iEEG) recordings from many brain areas (5), which have shown systematic spatial variation of instantaneous phases of the electrodes across the cortex. These systematic phase delays reveal the progressive propagation of neuronal activity across the cortex, known as *traveling waves*, which have been shown to be closely related to behavior (5).

Studies in animals showed that the frequency, strength, direction, and speed of traveling waves correlate with a broad range of behaviors in animals. These include visual perception (16-23), movement initiation (24-28), and memory processing (29, 30) in non-human primates as well as visual processing (31-33) and spatial navigation (34-36) in rodents. However, currently, there are no well-established methods for analyzing traveling waves in the human brain and rigorous computational tools specifically targeting the visualization and understanding of traveling waves are rare. Therefore, even though oscillations are seemingly ubiquitous in the human brain (2), many of the potential traveling waves associated with those oscillations have been missed. Although some iEEG studies in humans have demonstrated a role for traveling waves in cognition (5), systematic studies with rigorous analysis of traveling waves are still lacking.

In this chapter, our focus is on the development of novel approaches for the detection and analysis of traveling waves from human iEEG recordings. Most prior studies in the last two decades have detected traveling waves predominantly in scalp EEG and magnetoencephalography (MEG) recordings (37-42). However, several recent iEEG studies in humans have also demonstrated the existence of traveling waves (7-15). These iEEG recordings are from pharmaco-resistant epileptic patients who underwent neurological surgery for removal of their seizure onset zones. Traveling waves in these studies were usually detected and analyzed using the spatial gradient of the phases of the recordings from the iEEG electrodes (9, 12).

Traveling waves are present spontaneously during resting-state conditions such as eye-closure (9) (**Figure 1A**) and passive fixation (43) (**Figure 1B**). Traveling waves are also present during sleep spindles suggesting their putative role in memory consolidation and plasticity (8, 12) (**Figure 1C**). More recently, traveling waves were also detected during movement imagery suggesting their putative role in coordinating complex movements (13) (**Figure 1D**). Furthermore, traveling waves play a prominent role during speech processing (11), and also, during working memory, suggesting their putative role for memory processing as well (15) (**Figure 1E**).

To provide a broader introduction for how to measure traveling waves in the human brain, we describe an approach based on *circular statistics* to capture and analyze traveling waves amidst neuronal oscillations in iEEG recordings. Our approach overcomes several challenges for analyzing these waves in the human brain. First, we describe novel approaches for detecting oscillations in the iEEG electrodes and introduce methods to detect groups of nearby electrodes each having an oscillation at nearly identical frequencies. We then describe methods to detect and analyze the features of waves of electrical activity propagating across the cortex corresponding to these detected oscillations. We also introduce a novel approach based on circular statistics to track the progressive variation of the phases across multiple electrodes and subsequently detect traveling waves based on the fitted parameters of a circular-linear regression model. And, finally, we describe several features of the detected traveling waves and how they are intimately related with human behavior. Our approach is rigorous and can be used to identify multiple foundational mechanisms underlying the propagation of traveling waves and to reveal their link with behavior.

Approach to measure traveling waves of neuronal oscillations

Many previous studies of traveling waves in animal models used relatively simple analytical approaches based on the spatial gradient of phases. These approaches made sense because neural recording electrodes in animals are usually implanted in a relatively small area of the brain that was consistently placed across animals. However, there are several inherent aspects of human iEEG datasets that make it challenging to detect and analyze traveling waves. In particular, placements of electrodes across patients can be highly variable due to the complicated clinical protocols involved and can consist of multiple types of electrodes such as grid, strip, and depth electrodes (44, 45). Furthermore, the frequencies of neuronal oscillations can vary substantially across human patients, even after controlling for task behavior and electrode placement (15). Due to these challenges, an improved method for measuring traveling waves would be preferable if it were able to accommodate the specific features of the signals in a given patient’s iEEG recordings.

Our method overcomes these challenges by customizing the analysis pipeline according to the iEEG recordings from each individual patient (15, 43). This approach consists of two primary steps: (i) The first step consists of identification of spatially contiguous clusters of electrodes with narrowband oscillations at similar frequencies. Identifying a group of nearby electrodes with a single oscillation frequency is crucial since, by definition, a traveling wave involves a single frequency and whose phase progressively propagates through these electrodes, thus making it possible to detect the traveling wave when it passes by these electrodes. (ii) The second step consists of identification of systematic spatial variation of the instantaneous phases of the electrodes for each cluster, defined to be a traveling phase wave. This step is important since we want to capture the systematic phase delays of the wave across the group of electrodes in the oscillation cluster identified in step (i) above, thus enabling us to detect the presence or absence of a traveling wave. Once these systematic spatial variations in phases have been detected, we can then analyze the features of this spatial phase propagation and examine its relationship with human behavior. These procedures are detailed below. Our new approaches are flexible in the sense that they can be easily applied to other domains of brain imaging such as scalp EEG and MEG recordings as well as recordings from animal models.

Identification of oscillations and clustering algorithm

By definition, a traveling wave involves a neuronal oscillation that appears with a time delay across multiple regions of the cortex. Therefore, our first step in identifying these patterns is to detect oscillations that appear at a single frequency at multiple nearby electrodes. To detect such patterns, we first identify spatially contiguous clusters of electrodes with oscillations at the same or similar frequencies (15, 43). Critically, we perform this procedure in an adaptive fashion that is well suited for human iEEG data by accommodating differences in electrode positions and oscillation frequencies across individuals. This flexibility is especially important since iEEG electrodes in humans can be in the form of grid, strip, or depth electrodes and can also span multiple brain areas. Our approach can overcome this challenge by detecting waves which can travel through multiple types of electrodes and spanning many different brain areas, including both gray matter and white matter volumes.

The first step to detect oscillations in neuronal signals is estimating their power distribution in the frequency domain and distinguishing true narrowband rhythmic oscillations from background fluctuations such as the 1/f signal (15). There are several methods that can been used for such steps (15, 46, 47) (see also **Chapters 24 and 31**). In our work, we have used Morlet wavelets to compute the power spectra of the neuronal oscillations. Morlet wavelets are useful particularly for analyzing intracranial recordings because of their superior ability to detect transient, possibly non-stationary, oscillatory dynamics (15, 48). After using Morlet wavelets to measure each electrode's power spectrum, we then distinguish true narrowband oscillations as those that have peaks that are significantly greater than the background 1/f spectrum. We use a thresholding procedure to ensure that we specifically focus on significant narrowband oscillations that are reliably different from the background 1/f signal at an electrode (46).

We use this approach to identify narrowband oscillations at each recording site and eventually, to find multiple nearby electrodes oscillating at nearly the same frequency. To distinguish narrowband peaks in an electrode's power spectrum from the background signal, we fit a line to each patient's mean power spectrum in log–log coordinates using robust linear regression (15) (**Figure 2A**). We then subtract the actual power spectrum from the regression line. This normalized power spectrum removes the 1/f background signal and emphasizes narrowband oscillations as positive deflections (**Figure 2A.1**). We identify narrowband peaks in the normalized power spectrum as any local maximum greater than some predefined threshold. In our work (43), we used a threshold of one standard deviation above the mean, but other thresholds could be used depending on the experimenter's needs. This method reliably identifies the frequencies where individual electrodes show strong oscillations, as can be seen in **Figure 2A.1** which shows our approach from two example electrodes. One of these electrodes has a narrowband oscillation that we successfully detected at the theta frequency band and the other has one at alpha band, thus demonstrating the efficacy of this approach.

Next, to identify traveling waves (see below), we focus on the groups of contiguous electrodes that show oscillations at the same frequency. We focus on the contiguous electrode groups because our focus is to characterize the oscillations that are traveling waves by having each cycle propagating across contiguous regions of cortex. To identify these groups, or *oscillation clusters*, we implement a spatial clustering algorithm that we designed to find the contiguous groups of electrodes that exhibit narrowband oscillations at a given frequency (**Figure 2A.1**). To identify the specific electrodes that comprise a spatially contiguous group, we first create a pairwise-adjacency matrix that indicates whether each pair of electrodes is contiguous. This matrix indicates whether each electrode pair is separated by less than some predefined threshold (such as <= 20 mm (15)). Finally, we use this adjacency matrix to identify mutually connected spatial clusters of electrodes by computing the connected components of this graph (49). In our work, we only include clusters with at least four connected electrodes in our analysis. Further, in our work, we have allowed for some electrodes to show oscillations at nearby but nonidentical frequencies (such as within 10%; see (15)), which allows our procedure to accommodate oscillations that can slightly vary across frequencies. However, note that some parameters of this method could be tweaked according to the experimenter's needs. Once we identify a group of electrodes that oscillate at same or similar frequencies, we can then design methods to detect the presence or absence of a traveling wave. This is described below.

Identification of traveling waves

After identifying oscillation clusters in each person, which will distinguish the contiguous regions of cortex that oscillate at a single frequency, the next step in our framework is to identify traveling waves that propagate across that cluster (12, 15). Quantitatively, we can define a traveling phase wave as a set of simultaneously recorded neuronal oscillations at the same frequency whose instantaneous phases vary systematically with the location of the electrodes, such that individual cycles of the oscillation move across the cortex. A challenge for quantifying and tracking the traveling spatial patterns in human intracranial recordings is tracking the systematic presence of multiple cycles of oscillations across multiple electrodes. To perform this task, we use a circular-linear regression which models the relation between oscillation phase and electrode position (**Figure 2B**). Since the phase wraps around every 360 degrees, a circular-linear regression model, leveraging circular statistics (50), is important to use rather than a conventional linear model (**Figure 2B**).

To identify traveling waves from the phases of electrodes in each oscillation cluster (**Figure 2A.2**), we first measure the instantaneous phases of the signals from each electrode of a given cluster by applying a zero phase-lag filter at the peak frequency of the detected oscillation. In our analysis, we have used a Butterworth filter at the cluster's narrowband peak frequency (bandwidth [$f_p \times .85$, $f_p / .85$] where f_p is the peak frequency). We then use the Hilbert transform on each electrode's filtered signal to extract the instantaneous phase at each time-point of the iEEG recordings (15). However, other transforms such as the Fourier and wavelet transforms can also be used to extract the instantaneous phases of the electrodes as well. These instantaneous phase values are then fed-in to the circular-linear regression model described below.

In a traveling wave, the phases of an ongoing oscillation are spatially organized, with a systematic phase shift across space in the cortex. Accordingly, to measure such patterns, use a 2D circular-linear regression to quantitatively measure the relation between oscillation phase and electrode position. This regression lets us assess whether the observed phase pattern varies linearly with the electrode's coordinates (**Figure 2A.3**).

The structure for our circular-linear model is as follows. x_i and y_i represent the 2-D coordinates and θ_i the instantaneous phase of the ith electrode. Whereas the original electrode positions are of course in 3D in the brain's volumetric coordinates, we reduced the data to 2-D coordinates x_i and y_i corresponding to the cortical surface by projecting the 3-D Talairach coordinates of electrodes into the best-fitting 2-D plane using principal component analysis. Even though this procedure is most applicable to subdural grid electrodes, it can be applied to stereo EEG depth electrodes as well (43). This procedure can also be carried out in the 3-D volumetric space in the brain, however, projecting the 3-D coordinates to 2-D helps in better visualizing and interpreting the traveling wave (43). Based on the 2D electrode coordinates, to measure the phase propagation, we then fit a 2-D circular-linear model to the phase distribution at each timepoint. This model has the following structure,

$$\hat{\theta}_i = (a\, x_i + b\, y_i + \vartheta) \bmod 360^0,$$

where $\hat{\theta}_i$ is the predicted phase, a and b are the phase slopes corresponding to the rate of phase change (or spatial frequencies) projected into each of the orthogonal dimensions, and ϑ is the phase offset.

Circular–linear models do not have an analytical solution and, hence, we fit them iteratively using numerical methods (50), which makes this procedure computationally complex. To simplify model fitting, we first convert the parameters of the model from cartesian coordinates to polar coordinates. We define $\alpha = \text{atan2}(b, a)$ which denotes the angle of wave propagation and $\xi = \sqrt{a^2 + b^2}$ which denotes the spatial frequency (**Figure 2A.4**). We fit α and ξ to the distribution of oscillation phases at each time point by conducting a grid search over $\alpha \in [0^0, 360^0]$ and $\xi \in [0, 180/\delta]$ in sufficiently small increments of phase and phase/space steps respectively (for example, the step sizes used by (43) are 5° and 0.5°/mm for phase and phase/space respectively). Note that $\xi = 180/\delta$ corresponds to the spatial Nyquist frequency of $180/\delta$°/mm, corresponding to the highest spacing δ mm between neighboring electrodes. We fit the model parameters ($a = \xi\cos(\alpha)$ and $b = \xi\sin(\alpha)$) for each time point to most closely match the phase observed at each electrode in the cluster. We compute the goodness of fit as the mean vector length $\bar{r}$ of the residuals between the predicted ($\hat{\theta}_i$) and actual (θ_i) phases (50),

$$\bar{r} = \sqrt{\left[\frac{1}{n}\sum_{i=1}^{n}\cos\left(\theta_i - \hat{\theta}_i\right)\right]^2 + \left[\frac{1}{n}\sum_{i=1}^{n}\sin\left(\theta_i - \hat{\theta}_i\right)\right]^2},$$

where n is the number of electrodes. We choose the selected values of α and ξ to maximize $\bar{r}$. We repeat this procedure for each oscillation cluster. To measure the statistical reliability of each fitted traveling wave, we examined the phase variance that was explained by the best fitting model. To do this, we compute the circular correlation ρ_{cc} between the predicted ($\hat{\theta}_i$) and actual (θ_i) phases at each electrode (43):

$$\rho_{cc} = \frac{\sum_{i=1}^{n}\sin\left(\theta_i - \bar{\theta}\right)\sin\left(\hat{\theta}_i - \bar{\hat{\theta}}\right)}{\sqrt{\sum_{i=1}^{n}\sin^2\left(\theta_i - \bar{\theta}\right)\sum_{i=1}^{n}\sin^2\left(\hat{\theta}_i - \bar{\hat{\theta}}\right)}},$$

where bar denotes averaging across electrodes. Finally, to account for the variation in the number of electrodes across clusters, we apply an adjustment to control for number of fitted model parameters (43):

$$\rho_{adj}^2 = 1 - \frac{\left(1 - \rho_{cc}^2\right)(n-1)}{n-k-1},$$

where k is the number of independent regressors (k=3 in this case). We refer to ρ_{adj}^2 as the wave-strength of the traveling wave (15) as it quantifies the strength of the traveling wave (note that ρ_{adj}^2 has been referred to as phase gradient directionality (PGD) in some prior studies (12, 15, 26)). We note that ρ_{adj}^2 can now be compared across different clusters and subjects with varying number of electrodes. To test for the statistical significance of a traveling wave, we shuffle the coordinates of the electrodes and re-estimate the strength of the wave for each shuffling. In this way, we construct a histogram of surrogate wave-strength values against which we then compare the empirical wave-strength to test for the presence or absence of a traveling wave (43).

A step-by-step visual demonstration of the circular-linear regression approach to detect traveling waves has been illustrated in **Figure 3** for the iEEG recordings measured on two trials of a task, one with a traveling wave and the other without a wave. As a result of this fitting procedure, the direction α represents the spatial orientation at which the traveling wave propagates with a continuously increasing phase gradient through the cortex (**Figure 3**). When this direction α is visualized as an arrow on a brain plot, the traveling wave's propagation can be seen visually. In these plots, individual oscillation cycles appear at relatively early timepoints on the electrodes near the tail of the directional arrow and at later latencies on electrodes near the head of the arrow (**Figure 1A**).

Features of traveling waves

The 2D circular-linear model that we described above is a very useful quantitative tool for measuring the instantaneous properties of the traveling waves at each moment. The fitted coefficients a and b from the model can be used to calculate all the key features of the current traveling wave on that electrode cluster (**Figure 2A.4**). For example, the parameters α and ξ in the polar coordinates denote the angle of wave propagation and the spatial frequency respectively. Other features of the traveling wave such as the wavelength (2π/spatial frequency) and the speed (wavelength×frequency) can be readily derived from these parameters as well.

Another defining advantage of our proposed approach is that traveling waves can be reliably detected on a single-trial level using our methods. In a working memory task (15), we were able to detect traveling waves in ~81% of clusters at the single-trial level and ~67% of clusters had consistent traveling waves at the single-trial level which also had a consistent propagation direction. In another study using a verbal working memory task (51), we found that frontal theta and temporal alpha traveling waves are more reliably detected during the earlier periods of a trial compared to late detection of reliable temporal theta traveling waves in a trial, during the memory encoding periods.

Current studies have indicated that multiple features of traveling waves are related to human behavior (11, 51) (**Figure 4**). Traveling waves exist across a broad range of frequencies, starting from low frequency delta to higher frequency beta bands. Prior iEEG studies have detected traveling waves at alpha frequency during eye-closure resting-state in subdural grid electrodes (9), similar to the alpha waves observed in scalp EEG recordings (37). Recently, we have found traveling waves of theta and beta oscillations during passive fixation resting-state in the insula using stereo-EEG depth electrodes (43), indicating that traveling waves are present in not only the surface of the cortex, but also deep brain structures such as the insula. This finding also suggested that whereas lower frequency alpha oscillations are a defining feature of the resting brain at the surface of the cortex, higher beta frequencies may play an enhanced role in deeper structures of the cortex such as the insula. Other studies have also shown that these traveling waves are also highly relevant for memory processing in the human brain, and not just in resting-state. Specifically these studies have shown a crucial role for theta and alpha oscillatory traveling waves during a working memory task (15) and also verbal episodic memory task (51), suggesting that lower frequency oscillations might be more relevant for memory processing in the human brain. Some other studies have also shown a role of low frequency delta, theta, and alpha oscillatory traveling waves during speech processing as well (11). On the other hand, higher frequency beta oscillatory traveling waves play an important role during movement imagery (13) and sleep spindles (8, 12), in line with the role of beta frequency for sensorimotor neuronal activity processing and propagation of sleep spindles in the human brain, respectively.

The frequencies of these oscillations that we just described usually define the speed of propagation of traveling waves. Indeed, lower frequency traveling waves such as theta and alpha usually propagate in the range ~0.25-1 m/s (9, 15, 51), whereas higher frequency beta traveling waves usually propagate in the range ~0.5-5 m/s (12, 13). In our previous studies, we have also found that the speed of a traveling wave increases with an increase in its oscillation frequency (15). Moreover, prior work on computational modeling of weakly coupled oscillators has also shown that traveling waves can naturally emerge from spatially varying gradients of oscillations across different frequencies (52) and suggests that the propagation speed of these waves depends on the associated oscillation frequency. However, it is important to observe that these waves were detected using subdural grid electrodes on the surface of the cortex. In our more recent work, using stereo EEG depth electrodes, we have found that waves travel at ~0.7 m/s in the insula during passive fixation resting-state condition for both low frequency theta and higher frequency beta oscillations (43). This indicates that the speed-frequency relation of the traveling waves that we observe on the cortical surface may not be relevant for deep brain structures such as the insula and suggests that putatively different mechanisms might be involved for the origin of these traveling waves for the cortical surface and deeper cortical regions. Further studies are needed to definitively examine the speed-frequency relationship of these traveling waves. Rigorous computational models of these waves can go a long way in providing important insights into the characteristics of these traveling waves and the link between the different features of these waves. It is worth noting that, all these types of traveling waves features, and more, can be detected at each moment using the methods we described here.

Another important feature of a traveling wave is its propagation direction. The direction of a traveling wave informs us about the spatiotemporal coordination of different brain regions and its relation to behavior. In our previous studies, we have found that waves usually propagate from higher frequency regions to lower frequency regions (15), suggesting that the different features of traveling waves are inter-linked. More importantly, several studies have found that the propagation direction of these waves is linked to human behavior. The directions of traveling waves can distinguish speech compared to non-speech trials (11), successful memory encoding compared to unsuccessful memory encoding and memory recall in a verbal episodic memory task (51), and fast response times compared to slow response times in a working memory task (15), demonstrating its behavior relevance. Moreover, the directions of traveling waves also shift across brain regions. During eye-closure resting-state (9), waves travel from anterosuperior to posteroinferior direction broadly across the cortex. In a working memory task (15), the waves travelled from posterior to anterior direction in the frontal and temporal lobes, however no definite wave direction was found in the occipital and parietal lobes.

Furthermore, the timing (or phase) of traveling waves also plays a critical role in human cognition. In our recent study, we have shown that the timing of a wave precisely defines fast and slow response times, in a working memory task (51). These results may be similar to a set of findings in animals, where the phase of traveling beta oscillations predicted stimulus detection in visual perception (17).

Together, across this broad literature, these findings suggest that multiple features of traveling waves simultaneously define different behavioral states in humans. Since our proposed methodology can directly extract all these features of the traveling waves, it provides a useful tool for probing the direction of information flow for the precise spatiotemporal coordination of neuronal activity underlying different behaviors in humans.

Discussion

Oscillations play a prominent role in the brain and studies across multiple species have shown that they are correlated with learning, memory processing, and consciousness (1, 2). Even though oscillations are seemingly ubiquitous in the human brain (2), how these oscillations spatiotemporally coordinate neuronal activity across multiple brain regions, has remained elusive, due to lack of well-established methods for rigorously analyzing these oscillations. Recent advances (5) in obtaining highly precise, simultaneous intracranial EEG recordings from many brain areas have shown systematic spatial variation of instantaneous phases of the electrodes in an oscillation cluster which lays the foundation for possible existence of traveling waves. Intracranial recordings from subdural grid, strip, or depth electrodes often contain dynamics which are complex and it's difficult to visualize time-periods of systematic spatiotemporal patterns across broad regions in the brain and often, can be missed by separately analyzing individual traces of electrodes as is often done by neurologists (45). Using these types of traditional analysis, we can visualize the waves only when the recordings align with the direction of wave propagation and this may be the reason why many of the previous intracranial EEG studies might have missed these traveling waves (45), which are now known to be ubiquitous across the human brain (5). Traveling waves exist across multiple cognitive domains such as resting-state, speech, memory processing, and sleep, in the human brain, using iEEG recordings. Previous studies detected and analyzed traveling waves using the spatial gradient of the phases of the iEEG recordings (9, 12).

Here we described a new approach based on circular statistics to capture and analyze traveling waves in iEEG recordings. Our approach is general and can quantitatively measure all key features of these traveling waves. This approach consists of two primary steps, (i) identification of spatially contiguous clusters of electrodes, and (ii) identification of systematic spatial variation of instantaneous phases of the electrodes for each cluster, defined to be a traveling phase wave. Even though we described our approach in an iEEG setting, our methods are also applicable to other modalities such as scalp EEG, MEG, and optical recordings as well as field potential and depth electrode recordings in animals. These may be promising areas of future work because there is evidence for traveling waves in these settings as well (31, 34, 37, 53-55). Moreover, several features of traveling waves can be directly extracted from the parameters of our circular-linear regression model. We can then analyze the relationship of these features to different human behaviors as we have done in our previous studies (14, 15, 43, 51).

It is important to note that even with our analysis method, a number of features of the data must be satisfied in order to measure traveling waves. In particular, measuring traveling waves accurately requires adequate sampling of electrodes across the region that exhibits each oscillation. The detection of traveling waves is also constrained by the size of an oscillation cluster, and a sufficient number of electrodes, all oscillating at nearly similar oscillation frequencies, is necessary to capture a wave traveling across the cortex (15). To find the features of traveling waves that reliably correlate with behavior, owing to inter-individual differences in oscillations (15), a large sample size of patients may be important to reveal the key features of traveling waves. In one of our previous studies, we detected traveling waves across 77 patients in a working memory task (15), and we had found substantial heterogeneity in oscillation frequency and direction of these waves across patients. To this end, open-source data sharing efforts (see **Chapter 45**) will be crucial to analyze inter-individual and gender-related differences of traveling waves across large cohorts of patients.

Given that we found evidence for the existence of traveling waves across several frequency bands such as the delta, theta, alpha, and beta ranges (14, 15, 43, 51), it raises an important question of how the waves in these bands relate to each other. Previous studies have shown that theta and beta traveling waves in the human insula travel independently of each other during resting-state (43). In another study, gamma power was phase-locked to alpha traveling waves in the human neocortex (7), similar to the more traditional phase-amplitude coupling mechanism found in the human cortex (56). However, how the interactions of these waves in different frequency bands relate to human behavior remains unknown and future studies specifically focusing on developing novel methods for analyzing the interactions between these waves at different frequencies and their links to human cognition are needed to fill this important gap.

The new methods that we have developed related to traveling waves could potentially be informative about information coding in local neuronal activity and how it is coordinated across larger brain networks. Many brain areas that show traveling waves, including the hippocampus (14) and the neocortex (15), are also regions that show gradients in neural coding. Because the timing of local neuronal activity is phase-locked to specific phases of traveling waves (7, 47), it suggests that traveling waves may underlie neuronal processing by supporting a type of temporal multiplexing, in which only certain subregions in particular cortical areas are active at a given moment (57). We previously noted that traveling waves allow particular cortical regions to be consistently indexed by the phase delay of the overlying traveling waves, because human traveling waves maintain a consistent spatial frequency across trials (14). Combined with the findings that various cortical regions such as the hippocampus and the frontal lobe show gradients in neural representations that match the direction of traveling waves propagation (58, 59), this suggests that traveling waves could be important for large-scale information coding by allowing different cortical representations to be indexed at specific phase delays. Our rigorous approaches to precisely estimate the different features of traveling waves would thus be informative of a new type of cortical communication involving the role of traveling waves to coordinate cortico–hippocampal interactions.

It is also important to note that traveling waves also exist during interictal spiking activity (60) as well as seizures (61). It thus becomes critical to distinguish traveling waves arising from pathological activity from those arising from putative normal brain function, and further research is needed to develop more advanced methods for classification of normal and non-normal traveling waves (62). Finding strong relations between the different features of these traveling waves and human behavior may help to avoid interpretational difficulty between putative normal and pathological traveling waves.

Even though we focused on methods to detect and analyze planar traveling waves here due to their behavioral relevance (11, 15, 51), more complex patterns of traveling waves such as radial and spiral waves have also been detected in the human brain, especially during sleep spindles (8, 12), and also recently, in monkey (29, 63) and rodent (64, 65) brains. It will be interesting to show whether and how these more complex radial and spiral traveling waves are relevant for other types of behaviors such as learning, and verbal episodic and spatial memory tasks in humans. These complex patterns of traveling waves might also indicate excitation/inhibition of neural ensembles in the brain. For example, the center of an outward spiral or a source traveling wave might putatively have elevated neuronal excitation compared to the rest of the cortex and an inward spiral might have comparatively decreased neuronal excitation, in light of computational models that showed that traveling waves propagate from areas with faster intrinsic rhythmicity to the slower ones (52). This may help us identify brain regions with relatively distinctive levels of excitation/inhibition. Therefore, it is crucial to develop rigorous signal processing methods to carry out a comprehensive analysis of these complex patterns of traveling waves. Relatedly, some previous studies have suggested the use of curl and divergence analysis of spatial phase gradients to detect radial and spiral traveling waves (12, 31, 66, 67). Building on this work, an interesting future research direction would be to develop new methods by extending the circular-linear regression model-based methods presented here to account for more complex patterns such as radial or spiral waves or any combinations of these wave patterns. In our recent work, we have adopted the circular-linear regression approach described here to detect localized traveling waves by fitting the phase-plane in a localized sub-cluster of electrodes (**Figures 1B, 4A**) and shown that it is possible to estimate features of traveling waves for individual electrodes rather than the entire cluster of electrodes, and found more complex patterns of traveling waves beyond planar waves (43). Additional work is necessary to fully characterize the spatiotemporal features of these complex patterns of traveling waves, and this could provide a key step towards more fully distinguishing the functional role of the spatiotemporal dynamics of brain oscillations in various types of cognition.

References

1. Buzsáki G. Rhythms of the Brain. New York: Oxford University Press; 2000.
2. Buzsaki G, Draguhn A. Neuronal oscillations in cortical networks. Science. 2004;304(5679):1926-9.
3. Berger H. Über das Elektrenkephalogramm des Menschen. Archiv f Psychiatrie. 1929;87:527–70
4. Jasper H, Penfield W. Electrocorticograms in man: Effect of voluntary movement upon the electrical activity of the precentral gyrus. Archiv für Psychiatrie und Nervenkrankheiten. 1949;183:163–74.
5. Muller L, Chavane F, Reynolds J, Sejnowski TJ. Cortical travelling waves: mechanisms and computational principles. Nat Rev Neurosci. 2018;19(5):255-68.
6. Uhlhaas PJ, Pipa G, Lima B, Melloni L, Neuenschwander S, Nikolić D, et al. Neural synchrony in cortical networks: history, concept and current status. Front Integr Neurosci. 2009;3:17.
7. Bahramisharif A, van Gerven MA, Aarnoutse EJ, Mercier MR, Schwartz TH, Foxe JJ, et al. Propagating neocortical gamma bursts are coordinated by traveling alpha waves. J Neurosci. 2013;33(48):18849-54.
8. Dickey CW, Sargsyan A, Madsen JR, Eskandar EN, Cash SS, Halgren E. Travelling spindles create necessary conditions for spike-timing-dependent plasticity in humans. Nat Commun. 2021;12(1):1027.
9. Halgren M, Ulbert I, Bastuji H, Fabó D, Erőss L, Rey M, et al. The generation and propagation of the human alpha rhythm. Proc Natl Acad Sci U S A. 2019;116(47):23772-82.
10. Hangya B, Tihanyi BT, Entz L, Fabó D, Erőss L, Wittner L, et al. Complex propagation patterns characterize human cortical activity during slow-wave sleep. J Neurosci. 2011;31(24):8770-9.
11. Kleen JK, Chung JE, Sellers KK, Zhou J, Triplett M, Lee K, et al. Bidirectional propagation of low frequency oscillations over the human hippocampal surface. Nat Commun. 2021;12(1):2764.
12. Muller L, Piantoni G, Koller D, Cash SS, Halgren E, Sejnowski TJ. Rotating waves during human sleep spindles organize global patterns of activity that repeat precisely through the night. Elife. 2016;5.
13. Stolk A, Brinkman L, Vansteensel MJ, Aarnoutse E, Leijten FS, Dijkerman CH, et al. Electrocorticographic dissociation of alpha and beta rhythmic activity in the human sensorimotor system. Elife. 2019;8.
14. Zhang H, Jacobs J. Traveling Theta Waves in the Human Hippocampus. J Neurosci. 2015;35(36):12477-87.
15. Zhang H, Watrous AJ, Patel A, Jacobs J. Theta and Alpha Oscillations Are Traveling Waves in the Human Neocortex. Neuron. 2018;98(6):1269-81.e4.
16. Besserve M, Lowe SC, Logothetis NK, Schölkopf B, Panzeri S. Shifts of Gamma Phase across Primary Visual Cortical Sites Reflect Dynamic Stimulus-Modulated Information Transfer. PLoS Biol. 2015;13(9):e1002257.
17. Davis ZW, Muller L, Martinez-Trujillo J, Sejnowski T, Reynolds JH. Spontaneous travelling cortical waves gate perception in behaving primates. Nature. 2020;587(7834):432-6.

18. Gabriel A, Eckhorn R. A multi-channel correlation method detects traveling gamma-waves in monkey visual cortex. J Neurosci Methods. 2003;131(1-2):171-84.
19. Muller L, Reynaud A, Chavane F, Destexhe A. The stimulus-evoked population response in visual cortex of awake monkey is a propagating wave. Nat Commun. 2014;5:3675.
20. Nauhaus I, Busse L, Carandini M, Ringach DL. Stimulus contrast modulates functional connectivity in visual cortex. Nat Neurosci. 2009;12(1):70-6.
21. Townsend RG, Solomon SS, Chen SC, Pietersen AN, Martin PR, Solomon SG, et al. Emergence of complex wave patterns in primate cerebral cortex. J Neurosci. 2015;35(11):4657-62.
22. Vinck M, Lima B, Womelsdorf T, Oostenveld R, Singer W, Neuenschwander S, et al. Gamma-phase shifting in awake monkey visual cortex. J Neurosci. 2010;30(4):1250-7.
23. Zanos TP, Mineault PJ, Nasiotis KT, Guitton D, Pack CC. A sensorimotor role for traveling waves in primate visual cortex. Neuron. 2015;85(3):615-27.
24. Balasubramanian K, Papadourakis V, Liang W, Takahashi K, Best MD, Suminski AJ, et al. Propagating Motor Cortical Dynamics Facilitate Movement Initiation. Neuron. 2020;106(3):526-36.e4.
25. Denker M, Zehl L, Kilavik BE, Diesmann M, Brochier T, Riehle A, et al. LFP beta amplitude is linked to mesoscopic spatio-temporal phase patterns. Sci Rep. 2018;8(1):5200.
26. Rubino D, Robbins KA, Hatsopoulos NG. Propagating waves mediate information transfer in the motor cortex. Nat Neurosci. 2006;9(12):1549-57.
27. Rule ME, Vargas-Irwin C, Donoghue JP, Truccolo W. Phase reorganization leads to transient β-LFP spatial wave patterns in motor cortex during steady-state movement preparation. J Neurophysiol. 2018;119(6):2212-28.
28. Takahashi K, Kim S, Coleman TP, Brown KA, Suminski AJ, Best MD, et al. Large-scale spatiotemporal spike patterning consistent with wave propagation in motor cortex. Nat Commun. 2015;6:7169.
29. Bhattacharya S, Brincat SL, Lundqvist M, Miller EK. Traveling waves in the prefrontal cortex during working memory. PLoS Comput Biol. 2022;18(1):e1009827.
30. Zabeh E, Foley NC, Jacobs J, Gottlieb JP. Traveling waves in the monkey frontoparietal network predict recent reward memory. bioRxiv. 2022.
31. Liang Y, Song C, Liu M, Gong P, Zhou C, Knöpfel T. Cortex-Wide Dynamics of Intrinsic Electrical Activities: Propagating Waves and Their Interactions. J Neurosci. 2021;41(16):3665-78.
32. Stroh A, Adelsberger H, Groh A, Rühlmann C, Fischer S, Schierloh A, et al. Making waves: initiation and propagation of corticothalamic Ca2+ waves in vivo. Neuron. 2013;77(6):1136-50.
33. Xu W, Huang X, Takagaki K, Wu JY. Compression and reflection of visually evoked cortical waves. Neuron. 2007;55(1):119-29.
34. Agarwal G, Stevenson IH, Berényi A, Mizuseki K, Buzsáki G, Sommer FT. Spatially distributed local fields in the hippocampus encode rat position. Science. 2014;344(6184):626-30.
35. Patel J, Fujisawa S, Berényi A, Royer S, Buzsáki G. Traveling theta waves along the entire septotemporal axis of the hippocampus. Neuron. 2012;75(3):410-7.
36. Patel J, Schomburg EW, Berényi A, Fujisawa S, Buzsáki G. Local generation and propagation of ripples along the septotemporal axis of the hippocampus. J Neurosci. 2013;33(43):17029-41.

37. Alamia A, VanRullen R. Alpha oscillations and traveling waves: Signatures of predictive coding? PLoS Biol. 2019;17(10):e3000487.
38. Alexander DM, Jurica P, Trengove C, Nikolaev AR, Gepshtein S, Zvyagintsev M, et al. Traveling waves and trial averaging: the nature of single-trial and averaged brain responses in large-scale cortical signals. Neuroimage. 2013;73:95-112.
39. Lozano-Soldevilla D, VanRullen R. The Hidden Spatial Dimension of Alpha: 10-Hz Perceptual Echoes Propagate as Periodic Traveling Waves in the Human Brain. Cell Rep. 2019;26(2):374-80.e4.
40. Mahjoory K, Schoffelen JM, Keitel A, Gross J. The frequency gradient of human resting-state brain oscillations follows cortical hierarchies. Elife. 2020;9.
41. Massimini M, Huber R, Ferrarelli F, Hill S, Tononi G. The sleep slow oscillation as a traveling wave. J Neurosci. 2004;24(31):6862-70.
42. Zich C, Quinn AJ, Bonaiuto JJ, O'Neill G, Mardell LC, Ward NS, et al. Spatiotemporal organization of human sensorimotor beta burst activity. bioRxiv. 2022.
43. Das A, Myers J, Mathura R, Shofty B, Metzger BA, Bijanki K, et al. Spontaneous neuronal oscillations in the human insula are hierarchically organized traveling waves. Elife. 2022;11.
44. Mercier MR, Dubarry AS, Tadel F, Avanzini P, Axmacher N, Cellier D, et al. Advances in human intracranial electroencephalography research, guidelines and good practices. Neuroimage. 2022:119438.
45. Parvizi J, Kastner S. Promises and limitations of human intracranial electroencephalography. Nature Neuroscience. 2018;21(4):474.
46. Donoghue T, Haller M, Peterson EJ, Varma P, Sebastian P, Gao R, et al. Parameterizing neural power spectra into periodic and aperiodic components. Nat Neurosci. 2020;23(12):1655-65.
47. Watrous AJ, Miller J, Qasim SE, Fried I, Jacobs J. Phase-tuned neuronal firing encodes human contextual representations for navigational goals. Elife. 2018;7.
48. Solomon EA, Stein JM, Das S, Gorniak R, Sperling MR, Worrell G, et al. Dynamic Theta Networks in the Human Medial Temporal Lobe Support Episodic Memory. Curr Biol. 2019;29(7):1100-11.e4.
49. Tarjan R. Depth-first search and linear graph algorithms. Siam J Comput. 1972;1(2):146-60
50. Fisher NI. Statistical Analysis of Circular Data: Cambridge University Press; 1993.
51. Mohan UR, Zhang H, Jacobs J. The direction and timing of theta and alpha traveling waves modulate human memory processing. bioRxiv. 2022.
52. Ermentrout GB, Kopell N. Frequency plateaus in a chain of weakly coupled oscillators, I. SIAM journal on Mathematical Analysis. 1984;15(2):215-37.
53. Alexander DM, Nikolaev AR, Jurica P, Zvyagintsev M, Mathiak K, van Leeuwen C. Global Neuromagnetic Cortical Fields Have Non-Zero Velocity. PLoS One. 2016;11(3):e0148413.
54. Hindriks R, van Putten M, Deco G. Intra-cortical propagation of EEG alpha oscillations. Neuroimage. 2014;103:444-53.
55. Lubenov EV, Siapas AG. Hippocampal theta oscillations are travelling waves. Nature. 2009;459(7246):534-9.

56. Canolty RT, Edwards E, Dalal SS, Soltani M, Nagarajan SS, Kirsch HE, et al. High gamma power is phase-locked to theta oscillations in human neocortex. Science. 2006;313(5793):1626-8.
57. Friston KJ. Waves of prediction. PLoS Biol. 2019;17(10):e3000426.
58. Badre D, D'Esposito M. Is the rostro-caudal axis of the frontal lobe hierarchical? Nat Rev Neurosci. 2009;10(9):659-69.
59. Strange BA, Witter MP, Lein ES, Moser EI. Functional organization of the hippocampal longitudinal axis. Nat Rev Neurosci. 2014;15(10):655-69.
60. Smith EH, Liou JY, Merricks EM, Davis T, Thomson K, Greger B, et al. Human interictal epileptiform discharges are bidirectional traveling waves echoing ictal discharges. Elife. 2022;11.
61. Smith EH, Liou JY, Davis TS, Merricks EM, Kellis SS, Weiss SA, et al. The ictal wavefront is the spatiotemporal source of discharges during spontaneous human seizures. Nat Commun. 2016;7:11098.
62. Frauscher B, von Ellenrieder N, Zelmann R, Doležalová I, Minotti L, Olivier A, et al. Atlas of the normal intracranial electroencephalogram: neurophysiological awake activity in different cortical areas. Brain. 2018;141(4):1130-44.
63. Bhattacharya S, Donoghue JA, Mahnke M, Brincat SL, Brown EN, Miller EK. Propofol Anesthesia Alters Cortical Traveling Waves. J Cogn Neurosci. 2022:1-13.
64. Hamid AA, Frank MJ, Moore CI. Wave-like dopamine dynamics as a mechanism for spatiotemporal credit assignment. Cell. 2021;184(10):2733-49.e16.
65. Matityahu L, Gilin N, Atmna Y, Tiroshi L, Wickens JR, Goldberg JA. Mechanism of dopamine traveling waves in the striatum: theory and experiment. bioRxiv. 2022.
66. Ermentrout GB, Kleinfeld D. Traveling electrical waves in cortex: insights from phase dynamics and speculation on a computational role. Neuron. 2001;29(1):33-44.
67. Townsend RG, Gong P. Detection and analysis of spatiotemporal patterns in brain activity. PLoS Comput Biol. 2018;14(12):e1006643.

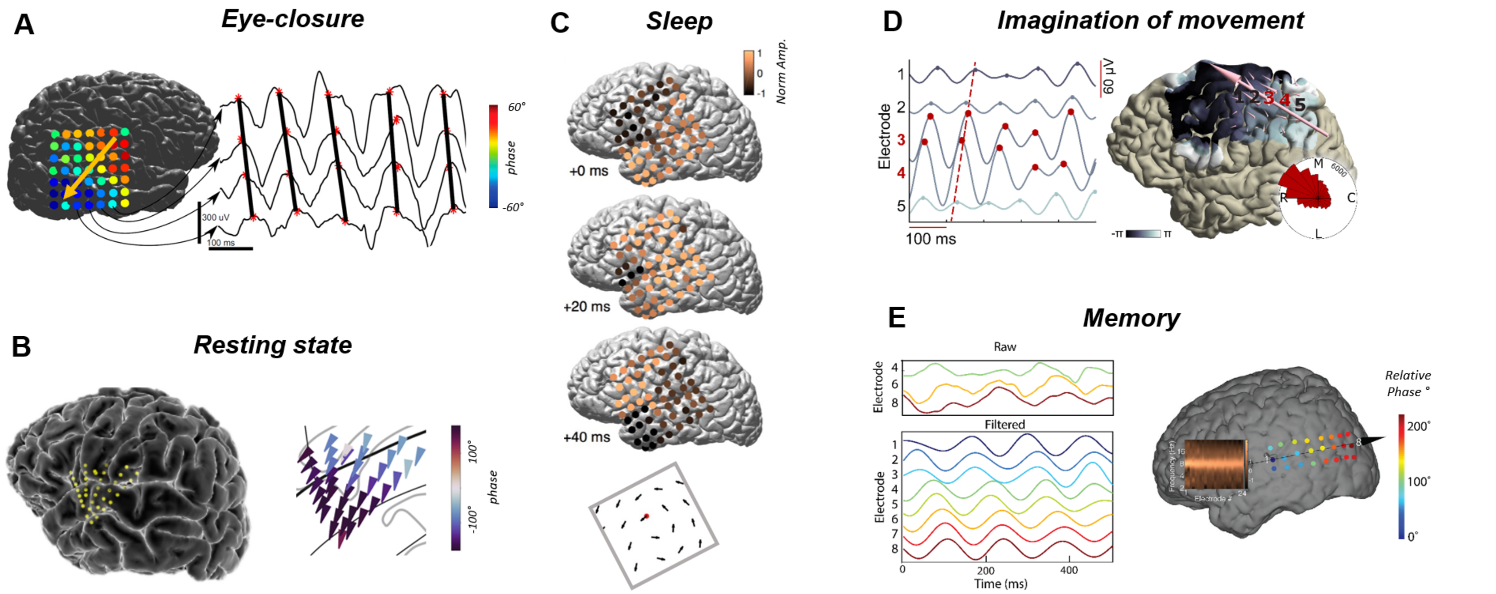

Figure 1. Traveling waves in the human brain across multiple domains, detected using iEEG. (A) Traveling waves during eye-closure resting-state condition. Alpha oscillations in patients propagated as traveling waves in the cortex during eye-closure resting-state condition. Colors of electrodes represent the phases of their oscillations (left panel) and traces represent the raw voltages of the marked electrodes (right panel). Adapted with permission from Halgren et al., 2019. **(B) Traveling waves during passive fixation resting-state condition in the insula.** Beta oscillations in the human insula propagated as traveling waves during passive fixation resting-state condition. Shown is an example of implanted stereo EEG electrodes in a patient (left panel), with arrows denoting the direction of the traveling wave associated with each electrode (right panel). Adapted with permission from Das et al. 2022. **(C) Traveling waves during sleep spindles.** Sleep spindles are traveling waves in the human brain. When visualized on the cortex, individual spindle cycles are often organized as rotating waves traveling from temporal (+0 ms, top) to parietal (+20 ms, middle) to frontal (+40 ms, bottom) lobes. Adapted with permission from Muller et al., 2016. **(D) Traveling waves during movement imagery in the sensorimotor cortex.** Alpha rhythmic activity during imagined movement in a representative individual. Shown are filtered signals for the five electrodes numbered on the brain plot (left panel). Cortical phase maps indicate the average phase at each cortical site relative to a central sensorimotor reference electrode. Local arrows indicate the propagation direction at each electrode, with arrow size weighted by the local phase gradient magnitude (right panel). Large global arrow indicates the mean propagation direction across the sensorimotor cortex, with arrow size weighted by the alignment of sensorimotor gradients. Alpha rhythm propagation is maximal in a caudo-rostral direction (red distribution, denoted by a polar plot). Adapted with permission from Stolk et al., 2019. **(E) Traveling waves during memory processing.** Alpha-theta oscillations are traveling waves in humans while performing a working memory task. Example shows data from a patient with an 8.3-Hz traveling wave (right panel). Shown are raw signals from three selected electrodes (left panel), the selected electrodes are ordered from anterior (top) to posterior (bottom). Also shown are the filtered signals (filtered at 6–10 Hz) for the eight electrodes numbered on the brain plot. Adapted with permission from Zhang et al., 2018.

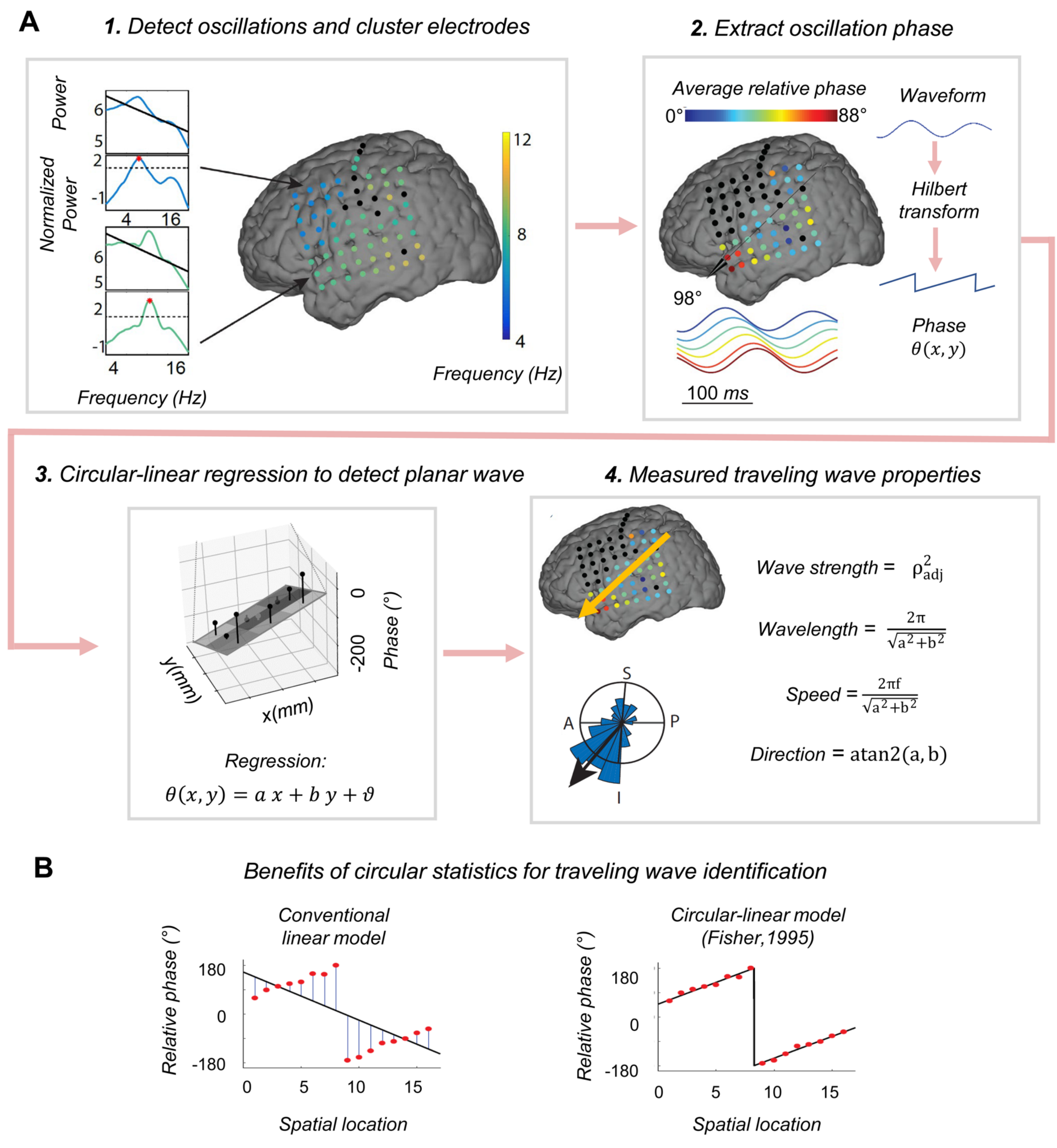

Figure 2. **Detection and analysis of traveling waves. (A) Flowchart illustrating the pipeline for detecting and analyzing traveling waves**. First column: Identification of spatially contiguous clusters of electrodes with narrowband oscillations at similar frequencies. Narrowband oscillation at each electrode was identified by fitting a line to each electrode's mean power spectrum in log–log coordinates using robust linear regression and then subtracting the actual power spectrum from the regression line. This normalized power spectrum removes the 1/f background signal and emphasizes narrowband oscillations as positive deflections. Shown are two oscillation clusters, one oscillating at theta frequency and the other at alpha frequency. Second column: Calculation of phases of the electrodes for each oscillation cluster. Phases of the oscillations were calculated using Hilbert transform on the filtered signals. Colors in this figure show the phases of the electrodes corresponding to the alpha oscillation cluster in the first column. Third column: Circular-linear regression was used to identify traveling waves of phase progression for each oscillation cluster at each time point. For each spatial phase distribution, two-dimensional (2-D) circular–linear regression was used to assess whether the observed phase pattern varies linearly with the electrode's coordinates in 2-D. Shown are solid circles representing the actual phases, the fitted plane, which is the predicted phase, and bars denoting the residuals between the actual and predicted phases. Fourth column: Features of traveling waves were calculated based on the fitted parameters of the circular-linear regression model. Shown are electrodes with colors denoting the phases and arrow denoting the direction of the traveling wave, with distribution of directions in blue, denoted by a polar plot. **(B) Advantages of the circular-linear regression model for the identification of traveling waves.** Due to the circular nature of the phase, any potential linear association between phase and electrode coordinates can be better estimated by the circular-linear model (right) compared to the linear regression model (left).

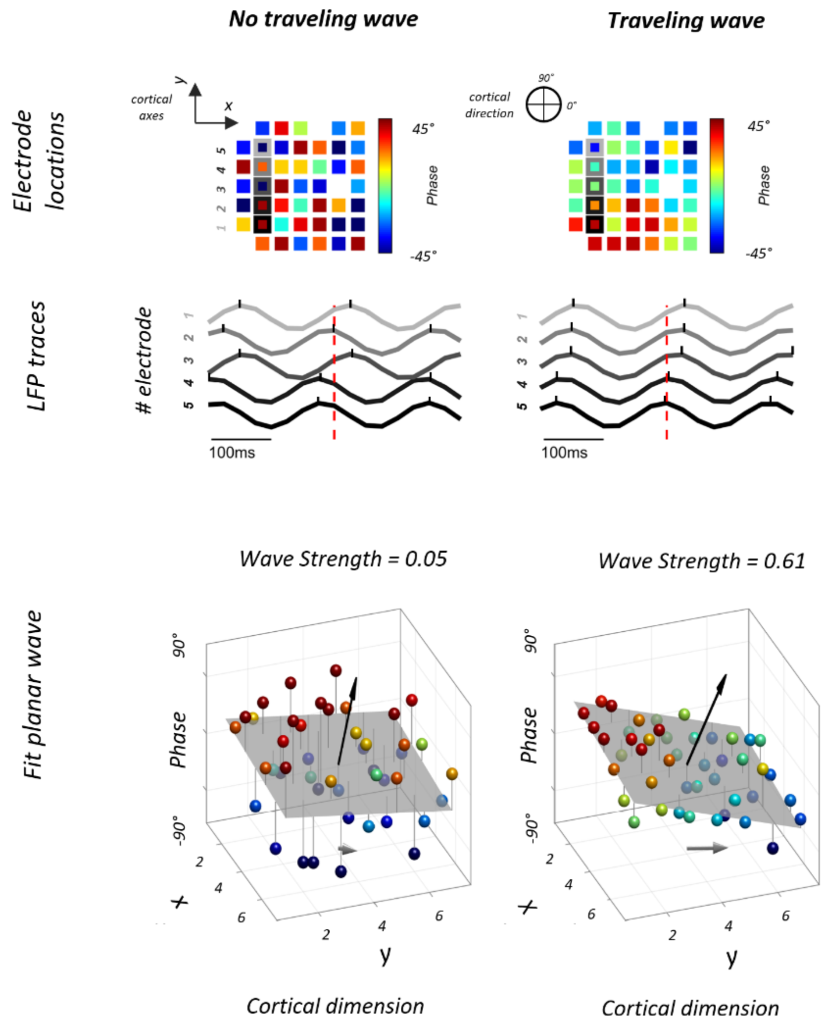

Figure 3. **Examples of detection of traveling waves for two representative trials.** Left and right columns correspond to two example trials demonstrating the absence and presence of a traveling wave respectively. Top row: Phase organization of electrodes in two representative trials of a cortical recording array with 49 electrodes. Colors represent the instantaneous phase of each electrode. Observe the systematic spatial variation of the phases of the electrodes in the right column indicating the presence of a traveling wave. Contrast this to the left column where there is no systematic spatial variation of the phases indicating the absence of a traveling wave. Middle row: Filtered LFP traces of five adjacent electrodes as labelled in the top row. Observe that the amplitude peaks occur at successively later times for electrodes 1-5 in the right column in contrast to the left column. Red-colored, vertical dashed lines represent the time-instants at which the phase distributions were plotted in the top row. Bottom row: Fitted planes estimated from the circular-linear regression analysis showing the best fit between the phases and the locations of the electrodes. Solid circles denote the actual phases of the electrodes with the colors as in the top-row and the vertical bars denote the residuals between the actual phases and the predicted phases using the circular-linear regression. The thick black arrows indicate the orthogonal vectors of the fitted planes and gray arrows represent the projection of these orthogonal vectors on the X-Y plane (cortical plane). Observe the smaller vertical bars in the right column indicating the presence of a traveling wave in contrast to the larger vertical bars in the left column indicating the absence of a traveling wave. Features of the traveling wave can be estimated by the parameters of the fitted plane (**Fig 2.A**).

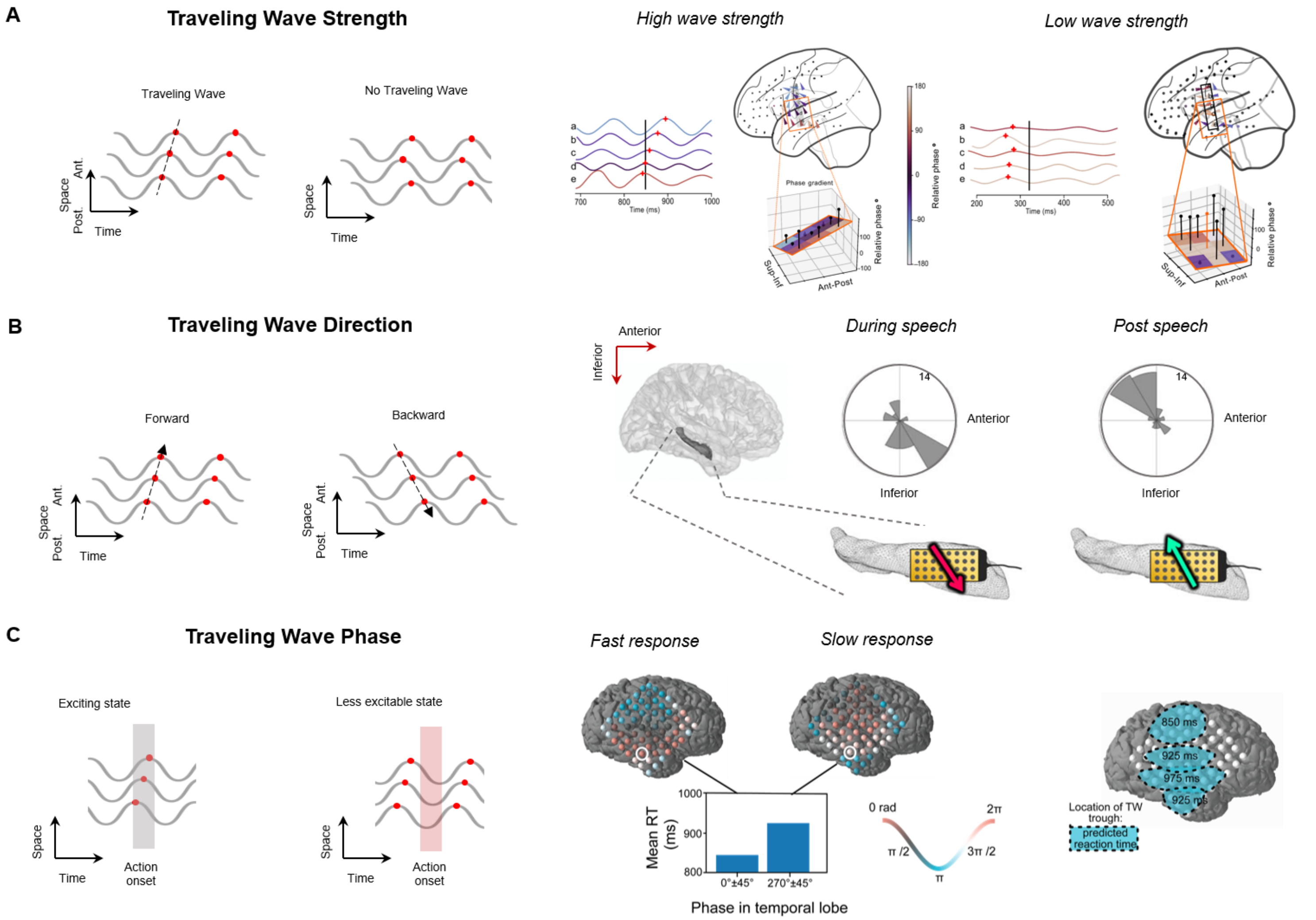

Figure 4. Features of traveling waves and potential behavioral relevance. (A) Wave-strength. (Left): Cartoon demonstration showing that systematic variation of the phase in space indicates high wave-strength, while non-systematic variation of phase indicates low wave-strength. (Right): Filtered signals of electrodes from two different trials (corresponding to the two different brain plots) from a representative patient performing a verbal episodic memory task, demonstrating high and low strength of traveling waves. Arrows denote the direction of the waves with colors denoting the phases. Note the lower residuals, indicating higher wave-strength in the first column, with higher residuals indicating lower wave-strength in the second column. In humans, no association has been found between wave-strength and behavior (51). Adapted with permission from Mohan et al., 2022. **(B) Direction.** (Left): Cartoon demonstration of forward and backward direction of traveling waves. (Right): iEEG recordings of the hippocampus from a patient demonstrating that the direction of traveling waves is dependent on the timing of a speech task, with waves traveling opposite to each other for speech compared to non-speech periods. Adapted with permission from Kleen et al., 2021. **(C) Phase.** (Left): Cartoon demonstration linking behavior to the phase of the traveling waves (excitable versus non-excitable). (Right): Recordings from electrocorticographic electrodes in a representative patient performing the Sternberg working memory task shows that the reaction time of the patient is correlated with the phase of the traveling wave in each electrode, shaping a spatial map for the preferred phase of the traveling wave for the optimal performance. Adapted with permission from Mohan et al., 2022.